



# Duffing Oscillator Model of Solar Cycles

Yury A. Nagovitsyn<sup>1,2</sup> and Alexei A. Pevtsov<sup>3</sup> 

<sup>1</sup> Central Astronomical observatory of Russian Academy of Sciences at Pulkovo, Saint Petersburg, 196140, Russia

<sup>2</sup> State University of Aerospace Instrumentation, Saint Petersburg, 190000, Russia

<sup>3</sup> National Solar Observatory, Boulder, CO 80303, USA; [apevtsov@nso.edu](mailto:apevtsov@nso.edu)

Received 2019 July 28; revised 2019 December 17; accepted 2019 December 18; published 2020 January 16

## Abstract

We propose that the solar cycle variability could be described in the framework of an external quasi-sinusoidal influence on an oscillator with cubic nonlinearity and linear damping (Duffing oscillator). To demonstrate this, we compare the empirical amplitude–frequency dependence with the theoretical one obtained by the Krylov–Bogolyubov averaging method. The empirical data are a composite time series of 2.0 version of sunspot number series, which starts in 1700, and the sunspot group number series by Svalgaard & Schatten, scaled to sunspot number, for 1610–1699 interval. We find that while this interpretation of solar cycle is a mathematical approximation, it explains several properties of solar cycle variability.

*Unified Astronomy Thesaurus concepts:* [Solar cycle \(1487\)](#); [Maunder minimum \(1015\)](#); [Analytical mathematics \(38\)](#)

## 1. Introduction

Understanding the solar and stellar activity cycles remains one of the fundamental questions of solar physics. In the earliest attempts to predict the solar cycles (e.g., Newcomb 1901), one of the main approaches was multi-harmonic analysis of past solar activity represented by sunspot number. This approach would identify the spectrum of amplitude and phase modulations, which then is used to predict the future solar activity. In one of the most recent examples, Zharkova et al. (2015) used the principle components analysis to infer the probability of incoming Grand Maunder-like Minimum.

The multi-harmonic analysis approach in predicting future solar activity is based on the assumption that solar activity is a repetitive process. This may not be the correct representation, as the solar activity has both periodic and stochastic components. Thus, for example, recent studies suggest that emergence of a large active region with peculiar orientation at the “right” phase of solar cycle may disrupt the surface flux transport and affect the strength of future cycles, including its complete shutdown (Nagy et al. 2017). The presence of a strong stochastic component in solar activity calls into question our ability to make correct predictions of long-term activity on the Sun, and whether the Sun (or a star) is entering or exiting a period of a grand (Maunder-like) minimum.

Current modeling of solar cycle variability employs several approaches, including direct numerical modeling (mean-field dynamo, full magnetohydrodynamics/MHD simulations, e.g., Charbonneau 2010; Pipin 2013; Labonville et al. 2019) and surface flux transport modeling (e.g., Upton & Hathaway 2018). The numerical modeling uses the prescribed flow patterns and their interaction with the magnetic field. The agreement with the observed properties of solar activity is achieved by varying several free parameters. Another strategy is to use the parameterized oscillator models, which allows us to investigate the effect of different parameters on properties of solar cycle. A review of this approach can be found in Lopes et al. (2014). The solar cycle exhibits several properties, which a good oscillatory model needs to address.

1. Variable strength and length of solar cycle: solar activity as measured by different proxies (sunspot or group number, area of sunspots etc.) shows periodic variations with quite different amplitude (e.g., sunspot number,  $SN = 81.2$  for cycle 6 and  $SN = 285.0$  for cycle 19) and period ( $P = 9.0$  yr for Cycle 2 and  $P = 13.7$  yr for Cycle 4 Takalo & Mursula 2018). There is a strong and statistically significant correlation between length of cycle  $n$  and amplitude of cycle  $n + 1$  (Solanki et al. 2002; Hazra & Nandy 2019). There is also weaker negative correlation between the amplitude and the period of the same cycle (Hathaway 2015).
2. Cycle asymmetry and amplitude: Waldmeier (1935) found that solar cycles exhibit an asymmetry between shorter duration rising phase (from sunspot minimum to maximum) and longer declining phase (from maximum to minimum). He also noticed a negative correlation between the length of rising phase of cycle and its amplitude: the shorter the ascending phase of cycle—the higher its amplitude although the correlation is not strong (Pearson correlation coefficient  $r = 0.83$ , Nagovitsyn & Kuleshova 2012).
3. “Lost cycle:” according to Gnevyshev & Ohl (1948, also see Nagovitsyn et al. 2009) for even–odd cycle pairs, areas under the cycle curve show statistically significant correlation. In odd–even cycle pairs, such correlation is not present. This led Gnevyshev & Ohl (1948) to conclude that true solar cycle is 22 yr (not 11 yr) especially, taking into account the reversal of leading polarity fields in sunspots in sequential cycles (Hale polarity rule, Hathaway 2015). Later, this led to development of a concept of magnetic cycle (Bracewell 1953). Gnevyshev & Ohl (1948) also noted that their rule has an exception—cycles 4 and 5 pair. However, if one assumes that between maxima of cycle 4 and cycle 5, there is an additional (“lost”) cycle with small amplitude (Usoskin et al. 2001), the Gnevyshev–Ohl rule is restored for all sunspot number data set including 17th century (Nagovitsyn et al. 2009). The “lost” cycle also appears in

the time–latitude (butterfly) diagram of sunspots in the declining phase of solar cycle 4 (Usoskin et al. 2009).

4. Rapid transitions from high to low amplitude cycles and the periods with suppressed amplitude of cycles: examples of such transition can be seen between cycles 4 and 5, cycles 9 and 10, and cycles 19 and 20. The pattern implies that there are periods when the amplitude of cycle steadily increases, and then decreases in a jump-like transition. Over the last 400 yr, there were two periods, the Maunder and Dalton minima, when the amplitudes of solar cycles were suppressed.

The asymmetry between ascending and descending phases of solar cycle and negative correlation between length of ascending phase and cycle amplitude suggest that the solar cycle is a nonlinear oscillatory system. Linear oscillatory systems do not show a correlation between amplitude and frequency of oscillations. For example, in mechanical linear oscillatory systems, the amplitude of oscillations depends on initial conditions, while the frequency is determined by a system’s elasticity. One of the nonlinear oscillators extensively applied in nonlinear dynamics is a Duffing oscillator with external forcing:

$$\ddot{x} + \omega^2 x + bx^3 + c\dot{x} = E \sin \nu t. \quad (1)$$

Within the framework of mechanical analogy, the term  $\omega^2 x + bx^3$  in Equation (1) describes nonlinear restoring force (per unit of mass),  $c\dot{x}$  is linear damping, and  $E \sin \nu t$  is external quasi-periodic perturbation.  $\omega^2 x$  and  $bx^3$  are the first and third terms of Maclaurin expansion for the nonlinear restoring force. The absence of a term with  $x^2$  implies that the restoring force is symmetrical. Fundamental oscillations of a system described by Equation (1) occur on frequencies of external excitation, which, in our case, defines the range of periodicity of solar cycles. The system can also give rise to subharmonic oscillations (e.g., Panovko 1980). With cubic nonlinearity, such as that in the Equation (1), the subharmonic oscillations will occur with the tripled basic frequency (with the quadratic nonlinearity, the basic frequency would double).

In some circumstances, a dynamical system represented by the Duffing equation may exhibit both cyclic and non-cyclic (chaotic) behavior (e.g., Cai et al. 2014; Li et al. 2019), which could be appropriate for modeling transitional states of solar cycle activity. Furthermore, the equation of the Duffing oscillator can be derived from the dynamo equations by their truncation (Lopes et al. 2014).

Restricting the restoring force expansion to the third-order terms corresponds to an oscillating system of weakly nonlinear-type. As the Equation (1) does not have the analytical solution, traditionally, the asymptotic techniques have been used. In general, the solutions of Equation (1) can be represented by the amplitude–frequency response curve, which is essentially a “portrait” of the system within the accepted approximation. Figure 1 provides a textbook example of amplitude–frequency response curve for Duffing oscillator as derived by Bogoljubov & Mitropolskij (1961, see also Mickens 1981). The portions marked by letters MAB and DCN on the response curve correspond to stable oscillations. The transitions BC and DA are where the oscillations are unstable. These transitions occur in points B and D, where the response curve has vertical tangents. As the frequency of oscillations increases from point M to point B (Figure 1), the amplitude of oscillations also increases. The amplitude at its highest value (a peak just before

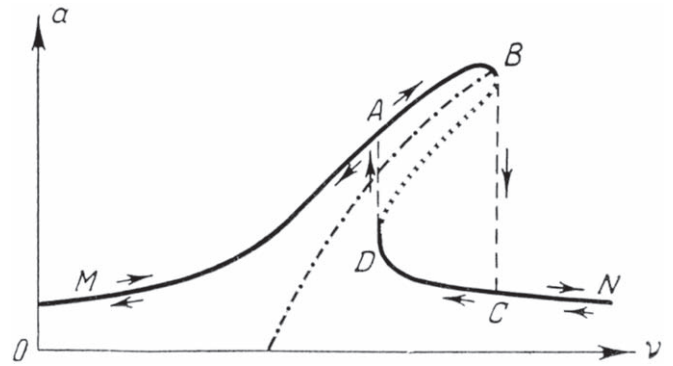


**Figure 1.** Amplitude–frequency response curve for Equation (1). The letters mark ranges of different regimes. The dotted–dashed line corresponds to the so-called “skeleton” curve, which corresponds to nonlinear free oscillations without external excitation. The solid line corresponds to stable solutions. The dotted line shows unstable solutions, and the dashed lines show jumps between stable solutions. The small arrows depict the evolution of a system along the response curve with increasing (arrows above solid curve)/decreasing (arrows below the curve) frequency. In this example, bending to the right corresponds to  $b > 0$  (see Equation (1)). The figure is a modified version of Figure 80 from the original monograph published in Russian in 1958; for an English translation see Bogoljubov & Mitropolskij (1961)

point B) corresponds to resonance oscillations. At point B, the system becomes unstable, and the amplitude jumps to point C. If the frequency continues increasing, the amplitude will decrease toward point N, but if the frequency starts decreasing, the amplitude will increase along segment CD. Reaching point D would result in a similar jump in amplitude of oscillations from point D to point A. The fact that BC and DA transitions do not coincide with each other is due to a hysteresis in the oscillator system. Depending on frequency changes, after the DA jump, the system may evolve either toward point M or toward point B (Figure 1). Without external forcing, the amplitude of oscillations increases with frequency along the dashed–dotted line shown in Figure 1. This amplitude–frequency dependence cannot explain the existence of two distinct oscillatory regimes on the Sun: regular cycles and periods of Grand minima, which, according to Usoskin et al. (2007), occurred 27 times over the last 12,000 yr. One should note that the alternative solution to the Duffing oscillator with external excitation could be an Van der Pol oscillator with stochastic parameters (Mininni et al. 2000; Lopes et al. 2014), which does not require an external excitation. However, to achieve the agreement with the observed properties of solar cycles, the Van der Pol–Duffing oscillator requires best-fit parameters of oscillator for each cycle (but see Mininni et al. 2000).

Here we use new sunspot data to investigate how well the solar cyclic activity may be described in the framework of a weakly nonlinear oscillatory system with an external periodic driver (i.e., Duffing equation). In a previous attempt to use the Duffing equation for interpreting solar cycle activity (Nagovitsyn 1997), the sunspot data were insufficient for representing a complete spectrum of solar cycle variations. Moreover, the level of solar activity for the 17th century based on Schöve (1955) was overestimated. Here we use the most recent sunspot number time series to show that the observed sunspot number time series fits the amplitude–frequency dependence of such an oscillatory system well. While this approach is an approximation, if successful, it could provide a path for developing a better understanding of jump-like transitions between high- and

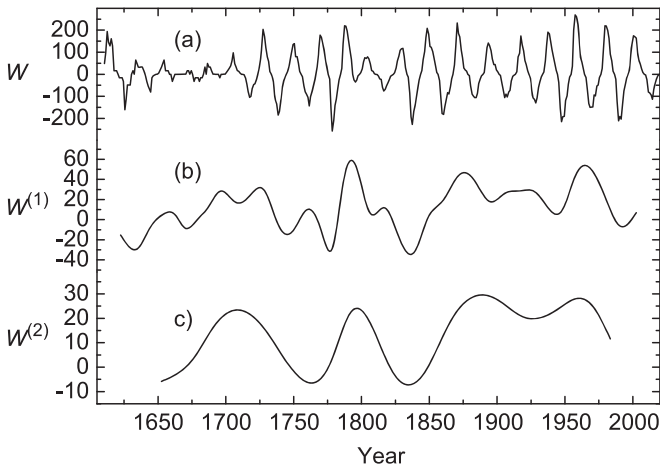


**Figure 2.** (a) Sign-alternating composite SN and GN time series (the time series used in this paper), and its first (b) and second (c) slow-varying components as derived in Section 2, Equations (4)–(5).

low-amplitude cycles, and identifying the incoming transition from a repetitive state (regular solar cycles) to activity during Maunder-type minima (e.g., cycles with extremely low amplitude, as recently discussed by Muñoz-Jaramillo 2019).

## 2. Data and Data Analysis

For the interval 1700–2017, we employ the annual values of 2.0 SN version from Clette et al. (2014). For the 1610–1699 interval, we adopt the Group Number (GN) series from Svalgaard & Schatten (2016). The two time series were combined using the relation  $\text{SN} = 18.3 \text{ GN}$  derived based on the period of overlap between the two data sets. During that period, annual SN and GN values show strong correlation (Pearson correlation coefficient  $\rho = 0.94$ ), which permits combining two data sets into a single one. In accordance with previous studies (see Section 1), on the declining branch of the fourth cycle we added a supplementary weak cycle with  $\text{SN} = 27$ . Instead of traditional unsigned series of sunspot numbers, we formed a time series with alternating signs. A signed time series has certain advantages for statistical analysis (e.g., zero mean), and it also takes into account the presence of the magnetic cycle. Figure 2(a) provides an example of the final time series used by us. Based on a visual analysis, it appears that the amplitude, which we selected to represent the “lost” cycle on the declining phase of the fourth cycle, fits the average maximum values of SN and GN during the Maunder minimum.

In order to estimate the frequency and amplitude of different components of the oscillations, we use the method proposed by Nagovitsyn (1997). The method is similar to empirical mode decomposition (Huang et al. 1998). To calculate frequencies and amplitudes for individual cycles (e.g.,  $j$ th cycle), we use the time moments  $T_j$  of cycles’ maxima and minima and sunspot number (Wolf number,  $W_j$ ) for these moments. Since our time series is represented by a signed SN, here “maxima” and “minima” refer to maxima of solar cycles in a traditional time series (Figure 2(a)). Then, we estimate the frequencies as

$$\nu_j = \frac{100}{T_{j+1} - T_{j-1}} \quad (2)$$

and amplitudes as

$$a_j = \frac{1}{4}(|W_j - W_{j-1}| + |W_{j+1} - W_j|). \quad (3)$$

In our formalism,  $\nu_j$  and  $a_j$  computed this way represent the “base” (or prime) component, which corresponds to an approximately 22 yr solar cycle periodicity.

For longer periods (longer than a solar cycle), we form a slow-varying additive component

$$W_j^{(1)} = \frac{1}{2} \left( \frac{W_{j+1} + W_{j-1}}{2} + W_j \right) \quad (4)$$

and

$$T_j^{(1)} = \frac{1}{2} (T_{j+1} + T_{j-1}). \quad (5)$$

Next, we smooth  $W_j^{(1)}$  and  $T_j^{(1)}$  by a cubic interpolation spline and use the resulting series to derive  $\tilde{W}_j^{(1)}$  and  $\tilde{T}_j^{(1)}$  using time moments of maxima and the corresponding SN the same way as in Equations (4) and (5).

In our formalism,  $\nu_j$  and  $a_j$  computed using original  $W_j$  and  $T_j$  (and Equations (2)–(3)) represent the “base” (or prime) component. Frequencies and amplitudes derived using  $\tilde{W}_j^{(1)}$  and  $\tilde{T}_j^{(1)}$  are the “first” component. The “second” components  $\tilde{W}_j^{(2)}$  and  $\tilde{T}_j^{(2)}$  are derived in a similar fashion as the “first” components but using time series of the “first” component. Figures 2(b)–(c) show “first” and “second” components of the original signed sunspot number time series (Figure 2(a)).

## 3. The Amplitude–Frequency Dependence

Using these three components of the original SN time series, we can now construct the amplitude–frequency dependence of the SN time series for different temporal shifts between frequency and amplitude. We find that the smallest scatter of points in an amplitude–frequency diagram can be achieved by the forward shift of frequencies, so the amplitude variations lag behind the variations of frequency by half of the 22 yr magnetic cycle. The amplitude–frequency dependence for such a forward shift is shown in Figure 3. There is a striking similarity between amplitude–frequency dependence derived from the observations and the response curve of the Duffing oscillator (compare Figures 1 and 3).

The amplitude–frequency dependence shown in Figure 3 implies that variations with shorter periods are followed by those with higher amplitudes. This is in agreement with Solanki et al. (2002), who found that the variations in length of solar cycle precede the changes in cycle amplitude. This behavior could be explained if we take into account that the damping term in Equation (1) that is the response to an external perturbation in dynamo process is transferred to the system for the time of the order of the 11 yr cycle rather than instantaneously. A corresponding rate of perturbation transfer can be estimated as  $k \cdot 10^5 \text{ km}/11 \text{ yr} = 0.3 \cdot \text{k}[m \text{ s}^{-1}]$ . If we evaluate the spatial scale of the cycle from the limits in which latitude drift of the spots occurs,  $0.7R_\odot$ , then the corresponding rate will be around  $1.5 \text{ m s}^{-1}$ ; evaluation from the width of the convective zone yields  $0.5 \text{ m s}^{-1}$ . Thereby the rate with which an external perturbation transfers its action to the oscillatory dynamo system lies between  $0.5$  and  $1.5 \text{ m s}^{-1}$ . For comparison, the amplitude of meridional flow typically

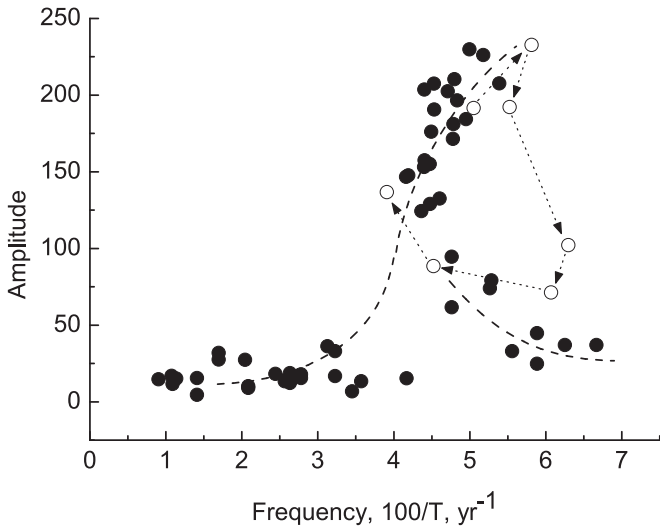


**Figure 3.** Empirical amplitude–frequency dependence for the sign-alternating SN time series (circles). The dashed line corresponds to MAB and NCD branches in Figure 1. The dotted line and open circles indicate activity during the Dalton minimum episode. Arrows mark the transitions, which appear similar to the BC and DA transitions in Figure 1.

used in surface flux transport simulations is about  $11 \text{ m s}^{-1}$  (Virtanen et al. 2017).

In Figure 3, open circles and arrows point out a Dalton minimum episode (end of 18th to start of 19th century), from cycle 2 to cycle 7. The far right point corresponds to the “lost” minor cycle on the branch of cycle 4. This behavior is close to the “breakdown” of the amplitude seen in Figure 1, when the amplitude reaches high values on the basic branch of amplitude–frequency relation of the Duffing equation with a further increase in external frequency. Note here that the extreme values for the “amplitude breakdown” are  $\nu_0 = 5.8$  and  $A = 240\text{--}250$ . The first value yields the upper limit for the frequency of cycles on the basic branch (Figure 1, reference point B), while the second restricts the amplitude of the cycles. The conclusions are as follows: first, that the amplitude of the cycles cannot be arbitrarily large, and second: when the frequency of the outer action exceeds, the dependence corresponds to the lower branch (D–N in Figure 1), that is, to global minima. In total, the experimental amplitude–frequency dependence of the solar cycle variability, derived from the alternating series SN, version 2.0, is close to theoretical for the Equation (1), and the solar variability may be represented as an oscillator (for example, traditional solar dynamo), excited by an outer quasi-sinusoidal force.

#### 4. Discussion and Conclusions

Using the first and second components of a composite (SN and GN) time series, we reconstructed the amplitude–frequency dependence of solar cycle variability. We show that it is similar in appearance to a weakly nonlinear Duffing oscillator. A derivation of the relationship between the dynamo equations and the equation for Duffing oscillator can be found in Lopes et al. (2014). Without going into the details, the left part of Equation (1) can be explained on the following grounds. The solar activity ( $x$ ) shows a quasi-periodic behavior, which can be represented by  $\ddot{x} = F(x, \dot{x})$  model. The asymmetry between the ascending and descending phases of the solar cycle and negative correlation between lengths of ascending phase and

cycle amplitude (e.g., Solanki et al. 2002) suggests that the solar cycle is a nonlinear oscillatory system. To represent this nonlinearity we can use the first and third terms of the Maclaurin expansion of function  $F$ . When limiting the expansion to the first and third terms, we assume that the system will have symmetric oscillations only. The historical records of sunspot activity do not show any indication of unlimited growth of amplitude of the solar cycle, which indicates that the oscillatory system should have a damping term. In the simplified case of a system with one degree of freedom, the damping force is  $\propto \dot{x}$ .

Past mathematical studies of the Duffing oscillator (e.g., Bogoljubov & Mitropolskij 1961; Panovko 1980) have demonstrated that without external excitation, the oscillator equation will show only one branch in the amplitude–frequency plot (the dashed–dotted line in Figure 1). The cyclic behavior during grand minima (dotted line in Figure 3) shows a change in amplitude–frequency behavior. In principle, such a change could be fitted without external forcing, but the fitting would depend on properties of each grand minima, and is likely to require different fitting parameters in Equation (1). Using external forcing (sin term in Equation (1)) allows creation of a unified fitting with only a single parameter, variable frequency.

While the identification of “forces” (or mechanisms) on the Sun, which could be associated with different terms of Duffing equation is outside the scope of current paper, we can provide some speculations in that respect.

The right side of Equation (1) describes an external disturbing force. One possible source of such external force might be planetary influence, such as, for example, the orbital period of planet Jupiter ( $P = 11.86 \text{ yr}$ ). Earth, Venus, and Jupiter alignments occur with a periodicity of  $11.07 \text{ yr}$ . Such closeness of planetary orbital periodicities to a period of a mean solar cycle was first noted by Wolf (1859). Recently, the effect of planetary orbital motions on the solar cycle was a subject of extensive discussions (see, for example, Abreu et al. 2012; Okhlopov 2016; Stefani et al. 2019, and references therein). However, the interpretation of observations in the framework of planetary influence on solar cycles was criticized by Poluianov & Usoskin (2014) and Holm (2015). Another possibility is that 22 yr variations in the polar field can serve such a role. One basis for such speculation is that a forward shift of about a half of the 11 yr cycle produces a similar amplitude–frequency dependence, as shown in Figure 3, albeit with slightly larger scatter as the 11 yr forward shift. However, half of the 11 yr cycle shift produces a much better defined transition between points B and C. The evolution of polar field may also provide an at least quantitative explanation for amplitude–frequency dependence (Figure 1). Naively, longer solar cycles may help with building stronger polar flux, which in turn would result in a subsequent solar cycle with higher amplitude (e.g., Pesnell 2008, 2016). This is, of course, is a gross simplification, as the strength of polar flux would depend on several other parameters, including the strength of the meridional flow, the flux emergence of active regions in mid-latitudes, and the strength of polar flux from the prior cycle.

Nevertheless, whether the planetary orbital or the polar field serves as an external perturbing force or there is another source requires additional investigation. The Duffing oscillator has one property that, perhaps, could be exploited in future studies, i.e., on the left side of the B–C jump, the external perturbation is in

phase with system oscillations, while on the right side of the jump, they are in anti-phase.

The nonlinear oscillator model explains several key properties of solar cycles (see, Section 1), including the variable amplitude and the length of the solar cycle, the asymmetry between ascending and descending phases of solar cycle, and negative correlation between length of ascending phase and cycle amplitude. The addition of the “lost” cycle of a very small amplitude to the declining branch of cycle 4 (Usoskin et al. 2001; Nagovitsyn et al. 2009) improves the appearance of a “breakdown” of the amplitude of oscillations from the high to low branch (D to C transition) characteristic of the Duffing oscillator (compare Figures 1 and 3). A reverse transition from periods of low Grand minima-type activity to regular cyclic variability also occurs in a jump-like fashion, albeit to the cycles with more moderate amplitude (D to A, Figure 1). The presence of jump-like transitions from a high to low amplitude cycle suggests that the maximum amplitude of solar cycles is limited. Once the system reaches that amplitude and frequency continues to increase, it transitions to a low-activity state, which may correspond to the grand (Maunder-like) minima. The existence of an upper amplitude limit for solar cycles is in agreement with the findings of Nagovitsyn et al. (2015). For a signed annual sunspot number time series, the amplitude of sunspot cycles is limited to about 240–250 SSN.

The purpose of this article is to demonstrate that mathematically, long-term variations in solar activity can be described in the framework of a nonlinear Duffing oscillator with external forcing. The authors recognize that the representation of solar activity in the framework of a Duffing oscillator is a simplification. However, we think, it could provide a path for developing a better understanding of jump-like transitions between high and low amplitude cycles.

This work has been partially supported by the Russian Foundation for Basic Research (RFBR) grant No. 19-02-00088 and Russian Academy of Sciences, Program No. 12. A.A.P. acknowledges a NASA NNX15AE95G grant. This work utilizes the sunspot number time series from WDC-SILSO, Royal Observatory of Belgium, Brussels. The authors thank the anonymous referee for their comments, which helped improve the article.

#### ORCID iDs

Alexei A. Pevtsov  <https://orcid.org/0000-0003-0489-0920>

#### References

- Abreu, J. A., Beer, J., Ferriz-Mas, A., McCracken, K. G., & Steinhilber, F. 2012, *A&A*, **548**, A88
- Bogoljubov, N. N., & Mitropolskij, J. A. 1961, *Asymptotic Methods in the Theory of Non-linear Oscillations* (New Delhi: Hindustan), 577
- Bracewell, R. N. 1953, *Natur*, **171**, 649
- Cai, M.-x., Yang, J.-p., & Deng, J. 2014, *Acta Math. Appl. Sin., Engl. Ser.*, **30**, 483
- Charbonneau, P. 2010, *LRSP*, **7**, 3
- Clette, F., Svalgaard, L., Vaquero, J. M., & Cliver, E. W. 2014, *SSRv*, **186**, 35
- Gnevyshev, M. N., & Ohl, A. I. 1948, *AZh*, **25**, 18
- Hathaway, D. H. 2015, *LRSP*, **12**, 4
- Hazra, S., & Nandy, D. 2019, *MNRAS*, **489**, 4329
- Holm, S. 2015, *Ap&SS*, **357**, 106
- Huang, N. E., Shen, Z., Long, S. R., et al. 1998, *RSPSA*, **454**, 903
- Labonville, F., Charbonneau, P., & Lemerle, A. 2019, *SoPh*, **294**, 82
- Li, X., Shen, Y., Sun, J., & Yang, S. 2019, *NatSR*, **9**, 11185
- Lopes, I., Passos, D., Nagy, M., & Petrovay, K. 2014, *SSRv*, **186**, 535
- Mickens, R. E. 1981, *An Introduction to Nonlinear Oscillations* (1st ed.; New York: Cambridge Univ. Press), 1
- Mininni, P. D., Gómez, D. O., & Mindlin, G. B. 2000, *PhRvL*, **85**, 5476
- Muñoz-Jaramillo, A., & Vaquero, J. M. 2019, *NatAs*, **3**, 205
- Nagovitsyn, Y. A. 1997, *AstL*, **23**, 742
- Nagovitsyn, Y. A., & Kuleshova, A. I. 2012, *ARep*, **56**, 800
- Nagovitsyn, Y. A., Nagovitsyna, E. Y., & Makarova, V. V. 2009, *AstL*, **35**, 564
- Nagovitsyn, Y. A., Obridko, V. N., & Kuleshova, A. I. 2015, *SoPh*, **290**, 1285
- Nagy, M., Lemerle, A., Labonville, F., Petrovay, K., & Charbonneau, P. 2017, *SoPh*, **292**, 167
- Newcomb, S. 1901, *ApJ*, **13**, 1
- Okhlopkov, V. P. 2016, *MUPB*, **71**, 440
- Panovko, I. G. 1980, *Introduction to the Theory of Mechanical Oscillations* (2nd ed.; Moscow: Nauka)
- Pesnell, W. D. 2008, *SoPh*, **252**, 209
- Pesnell, W. D. 2016, *SpWea*, **14**, 10
- Pipin, V. V. 2013, in *IAU Symp. 294, Solar and Astrophysical Dynamos and Magnetic Activity*, ed. A. G. Kosovichev, E. de Gouveia Dal Pino, & Y. Yan (Cambridge: Cambridge Univ. Press), 375
- Poluianov, S., & Usoskin, I. 2014, *SoPh*, **289**, 2333
- Schöve, D. J. 1955, *JGR*, **60**, 127
- Solanki, S. K., Krivova, N. A., Schüssler, M., & Fligge, M. 2002, *A&A*, **396**, 1029
- Stefani, F., Giesecke, A., & Weier, T. 2019, *SoPh*, **294**, 60
- Svalgaard, L., & Schatten, K. H. 2016, *SoPh*, **291**, 2653
- Takalo, J., & Mursula, K. 2018, *A&A*, **620**, 100
- Upton, L. A., & Hathaway, D. H. 2018, *GeoRL*, **45**, 8091
- Usoskin, I. G., Mursula, K., Arlt, R., & Kovaltsov, G. A. 2009, *ApJL*, **700**, L154
- Usoskin, I. G., Mursula, K., & Kovaltsov, G. A. 2001, *A&A*, **370**, L31
- Usoskin, I. G., Solanki, S. K., & Kovaltsov, G. A. 2007, *A&A*, **471**, 301
- Virtanen, I. O. I., Virtanen, I. I., Pevtsov, A. A., Yeates, A., & Mursula, K. 2017, *A&A*, **604**, A8
- Waldmeier, M. 1935, *MiZur*, **14**, 105
- Wolf, R. 1859, *MNRAS*, **19**, 85
- Zharkova, V. V., Shepherd, S. J., Popova, E., & Zharkov, S. I. 2015, *NatSR*, **5**, 15689